Desalination and Water Treatment
www.deswater.com
doi: 10.5004/dwt.2023.29962

310 (2023) 12–22
October

Productivity enhancement of solar stills using natural fibers: experimental investigation on the effect of *Strychnos potatorum* seeds and gooseberry stems

Chidambaram Muthiah[a,*], Sekar Subramani[a], Deepak Kumar Murugan[b]

[a]*Department of Mechanical Engineering, Rajalakshmi Engineering College, Chennai, India, Tel.: +91-9994013723; emails: muthiahct2003@gmail.com (C.T. Muthiah), sekar.s@rajalakshmi.edu.in (S. Sekar)*
[b]*Department of Mechanical Engineering, Velammal Engineering College, Chennai, India, email: deepu.energy@gmail.com (M. Deepak Kumar)*

Received 13 June 2023; Accepted 10 September 2023

ABSTRACT

Solar stills are a simple and renewable system for producing potable water from impure sources. However, the efficiency of solar stills is limited by their low productivity. Researchers have suggested various methods for improving the efficiency of solar stills, including the addition of natural fibers to the basin water. In this study, dried *Strychnos potatorum* seeds and dried gooseberry stems were added to the basin water to investigate their effect on productivity. The fibers were found to increase the surface area of the evaporating surface, which increases the rate of evaporation and overall productivity of the system. The dried *Strychnos potatorum* seeds and dried gooseberry stems have suitable porosity and solar absorption capacity, which further contribute to their effectiveness in enhancing the productivity of the solar still. The cumulative yield of the conventional solar still was found to be 1,053 mL/d, while the addition of *Strychnos potatorum* and gooseberry stem resulted in distillate outputs of 1,632 and 1,494 mL/d, respectively, corresponding to increases of 55% and 42%. Economic analysis indicated the feasibility of the process, making it a promising solution for sustainable and affordable water production. The observed increases in productivity could contribute to the widespread adoption of solar stills as a low-cost and sustainable method for producing potable water. These results demonstrate the potential of incorporating natural fibers into solar stills to improve performance and support the transition to sustainable water sources.

Keywords: Solar still; Natural fiber; Wick material; Solar distillation; Productivity enhancement; Solar desalination

1. Introduction

Water is an essential resource for life on earth, but unfortunately, water scarcity is becoming a growing concern worldwide. Water scarcity is a situation where the water demand exceeds the available supply of water. According to the United Nations, approximately 2.2 billion people worldwide lack access to safe drinking water, and this number is projected to increase due to climate change, population growth, and urbanization [1]. Water scarcity can severely affect human health, food security, and the environment [2]. In areas where water is scarce, people are often forced to drink contaminated water, spreading waterborne diseases such as cholera and typhoid [3]. Additionally, water scarcity can lead to malnutrition and starvation as crops fail due to a lack of water. Water scarcity also significantly impacts the environment, leading to the destruction of ecosystems, loss of biodiversity, and soil erosion. Desalination is an effective solution to overcome water scarcity as it allows the use of seawater, which accounts for 97.5% of the world's water resources [4]. This technology has become increasingly important in arid regions, where freshwater resources are

* Corresponding author.

limited and water demand is high. Desalination can provide a reliable source of freshwater, reducing the reliance on freshwater resources, which are often overused, leading to depletion [5,6]. Reverse osmosis (RO) is currently the most widely used desalination technology, accounting for approximately 60% of the world's desalination capacity. RO has several advantages over other desalination methods, such as low energy consumption and operating costs. Additionally, RO can produce high-quality freshwater, making it suitable for various applications, such as drinking, irrigation, and industrial uses. Desalination has several drawbacks to address to make it a sustainable solution to water scarcity. One of the main drawbacks is the high energy consumption required for desalination, which can be costly and contribute to greenhouse gas emissions. Additionally, desalination plants can harm marine life by discharging brine back into the ocean, leading to increased salinity and altered ecosystems. The disposal of brine also poses a significant challenge as it contains high concentrations of salt and other minerals.

Solar stills address the drawback of high energy consumption by conventional desalination technologies, using inexhaustible, clean, and free solar energy to generate heat and desalinate seawater [7,8]. Solar energy is a renewable energy source abundant in arid regions, making solar stills a sustainable solution to water scarcity. It is a simple device that uses solar energy to desalinate seawater [9]. It consists of a basin filled with seawater and covered with a transparent material, such as glass or plastic. The seawater is heated by the sun, causing it to evaporate. The water vapor condenses on the underside of the transparent material, forming freshwater droplets that flow down into a collection channel. Solar stills are relatively simple and easy to maintain, making them suitable for remote locations with limited access to technical expertise. Another advantage of solar stills is that they produce high-quality freshwater, making them suitable for various applications, such as drinking and irrigation. Solar stills also have minimal brine, reducing the impact on marine life and ecosystems.

Solar stills have several advantages over current desalination technologies and have the potential to provide a sustainable solution to water scarcity. However, despite their benefits, solar stills have yet to be widely commercialized. The major drawbacks of solar stills are their low productivity, land use requirements, and vulnerability to fouling [10–12]. Firstly, solar stills have lower productivity than other desalination technologies, such as reverse osmosis. The low productivity is due to the limitations of solar energy, which depends on weather conditions and the time of day. Solar stills require larger land areas to produce the same amount of freshwater as other desalination technologies, making them less cost-effective. Secondly, solar stills need a large land area to accommodate the large number of stills required to produce the necessary amount of freshwater. This can be a limiting factor in urban areas where land is expensive or unavailable. Moreover, the large land area requirements can negatively impact the environment, including habitat destruction and soil erosion.

Due to the burgeoning interest in this renewable energy system and its commercial viability, coupled with the pressing global need to address water scarcity issues, the solar still is receiving significant attention from researchers worldwide. Consequently, a myriad of studies is currently being conducted, marking an energetic drive towards creating innovative, green solutions to address the global issue. Various researchers inferred that the productivity of the solar still can be enhanced by increasing the evaporation rate of the feedwater. Many studies showed that the usage of energy storage material has significantly increased the productivity of solar still due to increase in evaporation rate [13–16]. An inclined wick solar still increases evaporation rate and condensation efficiency, leading to potentially higher water output due to enhanced heat absorption and minimized heat loss. Commonly used wick materials in solar stills include cotton, synthetic fibers (such as polyester or nylon), and cellulose-based materials (like paper or wood). These materials are chosen for their absorbent properties, capillary action, and availability [17–20]. Recent advancements in solar desalination research underscore the transformative role of porous absorber layers. Multiple studies have consistently highlighted its efficacy in augmenting system performance across various configurations [38–40]. Researchers have also explored the use of multiple wick solar stills, which employ more than one wick for enhanced water evaporation and condensation. Common materials utilized in multiple wick solar stills include cotton, jute cloth, charcoal cloth and wool fibres [21–23].

In this research study, the effectiveness of incorporating natural fibers, specifically dried *Strychnos potatorum* seeds and dried gooseberry stems, into solar stills to improve their efficiency and productivity. The observed increase in productivity, as high as 55%, highlights the potential of this technique for wider adoption in water-scarce regions and for emergency relief situations. Moreover, the economic analysis shows that the process is feasible, further supporting its potential as a viable solution for sustainable water production. The use of these natural fibres in solar stills is a novel approach that has not been extensively explored, and this study provides valuable insights into the benefits of this technique. The results of this research have significant implications for addressing the global water crisis, and could contribute to the transition towards sustainable and affordable water sources. This work represents a significant contribution to the field of solar stills and water production, and provides a foundation for future research on this promising approach.

2. Materials and methods

2.1. Characterization of the fibre

In this section, the theoretical models employed to characterize the natural fibres are presented. The performance of these fibres is evaluated based on their porosity, capillary rise and water absorbency. Theoretical models are employed to quantify these properties and the suitability of these natural fibres for solar distillation applications is discussed.

2.1.1. Porosity

Porosity (ε) represents the void fraction within a fibrous material and is crucial in determining the wicking performance of the fibres. The porosity can be calculated by comparing the bulk volume (V_b) and solid volume (V_s) of the material, as given by the following Eq. (1) [24]:

$$\varepsilon = \frac{\left(V_b - V_s\right)}{V_b} \tag{1}$$

The porosity of *Strychnos potatorum* and gooseberry stem are estimated to be 34% and 47%, respectively. The latter has a better porosity due to the presence of hydrophilic components like cellulose and hemicellulose.

2.1.2. Capillary rise

Capillary rise (h) is a key property that influences the water transport ability of the fibres in a solar still. Jurin's Law is utilized to estimate the capillary rise, as shown in Eq. (2) [25]:

$$h = \frac{\left(2 \times \sigma \times \cos\theta\right)}{\left(\rho \times g \times r\right)} \tag{2}$$

where σ is the surface tension of the liquid (N/m), θ is the contact angle between the liquid and the fibre surface (°), ρ is the density of the liquid (kg/m^3), g is the gravitational acceleration (9.81 m/s^2), and r is the radius of the capillary (m). The capillary rise of *Strychnos potatorum* and gooseberry stem are 8.2 and 12.4 mm/h, respectively.

2.1.3. Water absorbency

Water absorbency rate (W_{rate}) is an essential characteristic for assessing the speed at which fibres attain their maximum water-holding capacity. It can be evaluated by measuring the time taken for the fibres to reach their maximum absorbency which can be determined using the weight difference between the wet (W_w) and dry (W_d) samples, as described by Eq. (3) [26]:

$$W = \frac{\left(W_w - W_d\right)}{W_d} \tag{3}$$

The water absorbency rate of *Strychnos potatorum* and gooseberry stem are 6s and 4s, respectively.

2.2. Solar still system description

In this study, we aimed to design and construct a highly efficient solar thermal water heating system using readily available materials. The basin material was carefully selected to be made of wood due to its low thermal conductivity of 0.12 W/m·K. The rationale behind this choice was to minimize heat loss to the surroundings and thereby improve the overall efficiency of the system. To further enhance the insulation properties of the basin, glass wool was used as an insulating material at the bottom so that heat is not lost to the ground surface through conduction. With a thermal conductivity of 0.0343 W/m·K, the glass wool significantly reduced heat transfer through the bottom of the basin. To ensure efficient transfer of heat to the water, aluminium sheets were placed on the inner side walls of the basin. The aluminum sheets placed on the inner side walls of the basin not only absorb solar radiation and transfer heat to the water, but they also reflect the solar radiation that is reflected from the surface of the water back towards the water. This feature of the aluminum sheets further improves the efficiency of the system by ensuring that more of the solar radiation is absorbed by the water, rather than being lost to the surrounding environment. At the bottom of the basin, a galvanized sheet metal painted black was placed as the absorber plate to maximize solar radiation absorption. The galvanized sheet metal was chosen due to its good water corrosion resistance, ensuring the system's longevity. Finally, silicon sealants were used to seal the system and avoid vapor leakage. It is crucial to seal the system properly to prevent energy loss due to vaporization and ensure the system's efficient operation. The schematic diagram of the experimental setup is as shown in Fig. 1. The condensing cover of the solar still was selected to be made of glass due to its excellent transparency and ability to transmit solar radiation [27]. Additionally, glass is easily available and has the added benefit of reflecting re-emitted radiation, further improving the system's efficiency. To optimize the

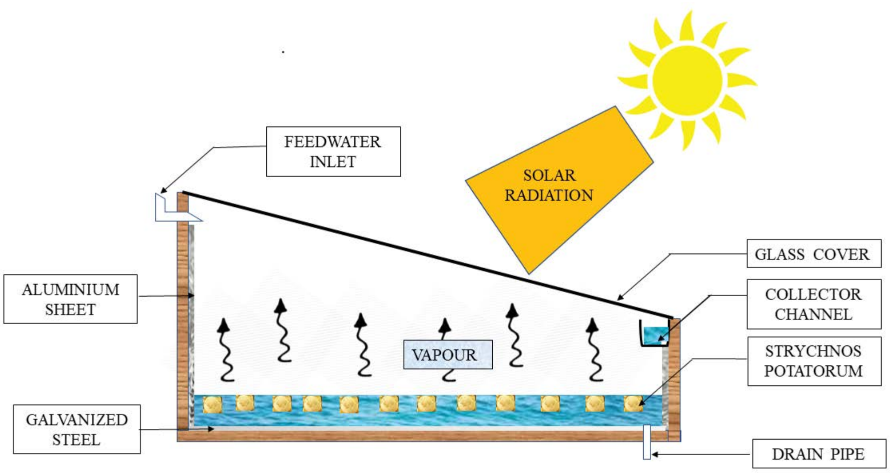

Fig. 1. Schematic diagram of the solar still set-up.

angle of the condensing cover for the specific geographic location of the system, the inclination angle was set to be equal to the latitude angle of 13° [28]. This angle was carefully selected to ensure that the system received the maximum amount of solar radiation possible, thus improving its overall performance.

2.3. Uncertainty analysis

Experimental uncertainty is a critical aspect of any scientific research as it is essential to accurately evaluate and quantify the precision and accuracy of the measurements and results obtained. The uncertainty provides valuable insight into the reliability and validity of the experimental data and helps to assess the degree of confidence that can be placed in the findings. Uncertainty is defined as the measure of the range of values within which the true value of the measured quantity is expected to lie. In the context of a solar still system, the uncertainty is the measure of the precision and accuracy of the measurements obtained from the various instruments employed in the experiment. The various instruments employed in this research work are solarimeter, anemometer, thermocouple, and measuring flask. The solarimeter is used to measure the solar radiation, while the anemometer measures the wind speed. The thermocouple is used to measure the temperature, and the measuring flask is used to measure the volume of water.

The proportion of an instrument's minimum discernible value to its lowest observable output measurement is a prevalent method for characterizing the instrument's uncertainty [29]. The assorted uncertainties linked to the measuring devices are detailed in Table 1. Owing to the various uncertainties inherent in these instruments, the subsequent equation has been employed to approximate the uncertainty in the solar still's distillate production [30]:

$$U_x = \sqrt{\left(\frac{\partial X}{\partial x_1}U_1\right)^2 + \left(\frac{\partial X}{\partial x_2}U_2\right)^2 + \dots\dots\dots\left(\frac{\partial X}{\partial x_n}U_n\right)^n} \quad (4)$$

where U_x signifies the uncertainty associated with the solar still's yield, while U_n denotes the uncertainty pertaining to the measuring instruments.

2.4. Experimental procedure

The present study analysis of the effect of organic absorbents on the productivity of solar still and the results are compared with the conventional solar still to evaluate the performance. The tests were carried out in the months of June, July and August, 2022 at Rajalakshmi Engineering College, Chennai, India (latitude and longitude of 13.0009°N and 80.1194°E). The solar still was positioned towards the south direction to capture maximum solar radiation. The experiments were carried out for a duration of 10 h starting at 0800 h in the morning and ending at 1800h in the evening. The freshwater yield of the conventional solar still is measured and then the effect of adding the organic absorbents such as *Strychnos potatorum* and gooseberry stem is analysed. The various operating conditions such as solar radiation intensity, wind velocity, ambient temperature, basin, water and glass cover temperatures are measured. The measurement stability was affirmed by repeating each separate test cases many days on a similar meteorological condition so as to ensure that the effect of adding these absorbents alone is analysed. The photograph of the experimental setup is shown in Fig. 2.

The solar radiation gets transmitted through the transparent glass cover and reaches the side walls of the basin and the water surface. The absorber plate kept at the bottom absorbs heat and transmits it to the water through convection. The water then evaporates and condenses on the inner side of the glass cover. The inclination angle of the condensing cover facilitates the collection of distilled potable water on to a separate collecting channel. In case of the solar still with absorbents, the evaporation rate of the water surface is enhanced by increasing its surface area with the aid of the absorbents which acts as an organic wick material due to its porous structure. The absorbents are added to the basin water to ensure that the top surface of water is covered with them to enhance the surface area and evaporation rate.

In evaluating the performance of the solar distillation system, the efficiency (η_d) was ascertained using Eq. (5) [34]:

$$\eta_d = \frac{\sum m_w \times h_{fg}}{A \times I(t)} \quad (5)$$

where m_w denotes the daily distillate yield, h_{fg}, is the latent heat of vaporization, A symbolizes the base area of the still, and $I(t)$ is representative of the mean incident solar radiation over the specified duration.

3. Results and discussion

3.1. Variation of solar radiation intensity

The performance of solar stills is inextricably linked to the variation in solar radiation intensity throughout the day. The conversion of brackish water into potable water is primarily driven by the energy harnessed from the sun.

Table 1
Instrument uncertainties

Instrument	Accuracy	Least count	Range	Uncertainty (%)
Thermocouple	±0.1°C	0.1°C	0°C–100°C	0.7
Pyranometer	±10 W/m^2	1 W/m^2	0–2,500 W/m^2	2.7
Anemometer	±0.1 m/s	0.1 m/s	0–32 m/s	2.4
Measuring jar	±5 mL	1 mL	0–500 mL	1.6

Consequently, the impact of solar radiation intensity on the efficiency of solar stills is vital for optimizing their design and operation. The efficiency of a solar still is determined by the effectiveness of the energy transfer from solar radiation to the saline water within the still. This transfer occurs through several mechanisms, including direct absorption by the water, reflection, and transmission through the glazing material. Throughout the day, the intensity of solar radiation undergoes fluctuations, as shown in Fig. 3. Early in the morning, around 0800h, the radiation intensity is relatively low, measuring approximately 310 W/m^2. As the day progresses, this intensity escalate, eventually peaking at about 920 W/m^2 by 1300 h. Subsequently, the intensity undergoes a gradual decline, settling around 400 W/m^2 by 1800 h. As the solar radiation intensity increases, the rate of evaporation rises, leading to enhanced production of freshwater vapor. This vapor then condenses on the cooler glazing surface, eventually trickling down into a collection reservoir as potable water. However, as the solar radiation intensity diminishes towards the evening, the temperature gradient decreases, thereby reducing the rate of evaporation and, subsequently, the freshwater yield.

3.2. Transient temperature variations

The measured variations of temperature at different positions in a solar still, such as basin, feedwater, inner glass cover, and the surrounding, is presented in Figs. 4 and 5. The glass, water, absorber, and ambient temperatures were recorded for each configuration at various time points, starting at 0800 h and concluding at 1800 h. The temperature trends for all three configurations show a

Fig. 2. Photograph of the experimental set-up.

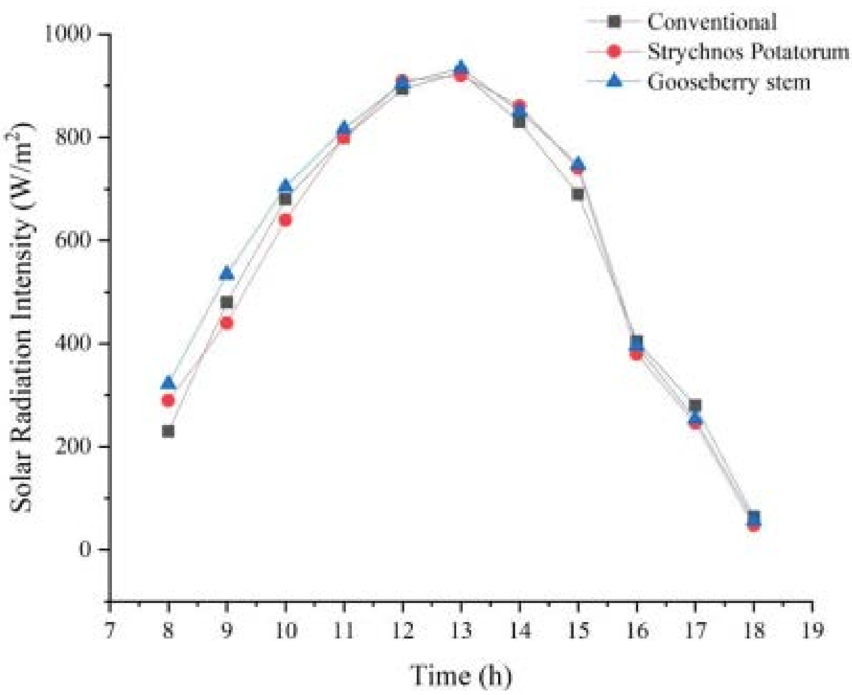

Fig. 3. Solar radiation intensity for the experimental time period.

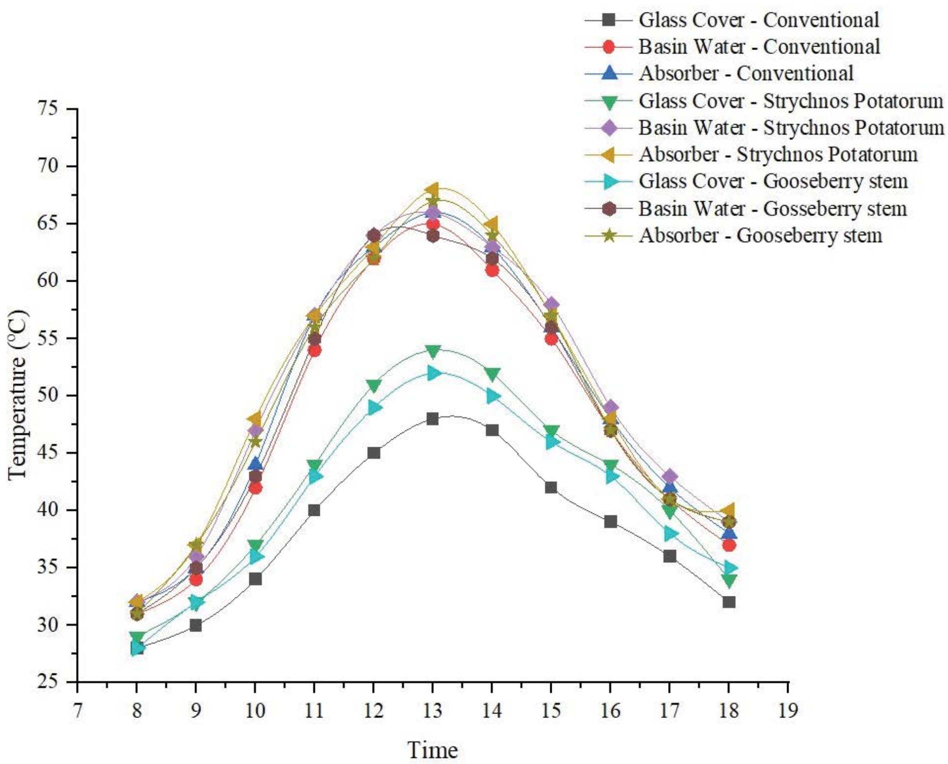

Fig. 4. Transient temperature variations of glass cover, basin water and absorber of all the configurations.

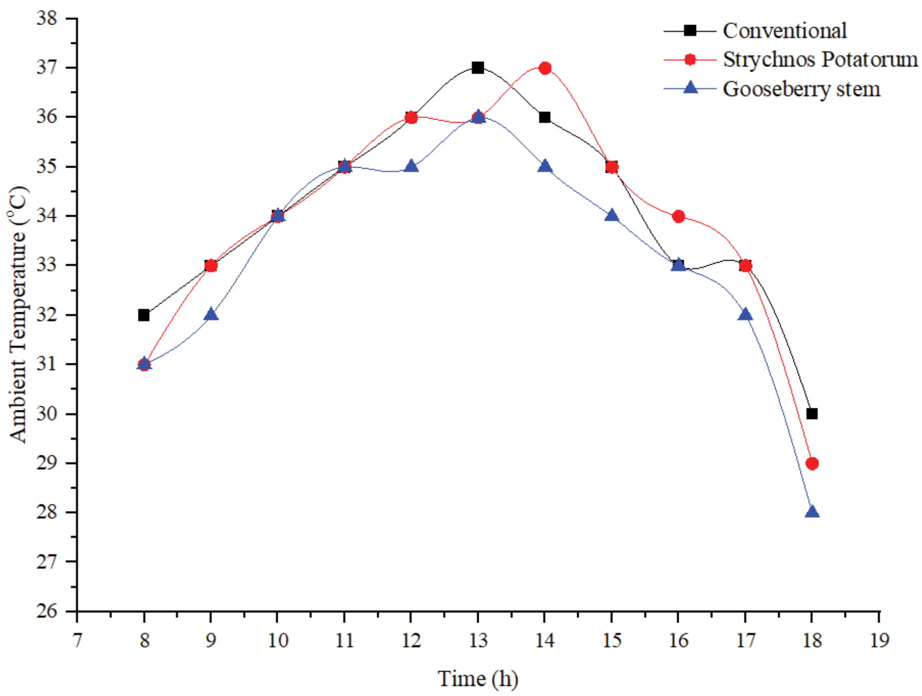

Fig. 5. Hourly variation of ambient temperature.

similar pattern: an increase during the morning hours, a peak around midday, and a subsequent decrease towards the evening. This pattern can be attributed to the diurnal variation of solar radiation, which reaches its maximum intensity around noon, and the greenhouse effect created by the glass cover, which traps the long-wave radiation emitted by the water, basin, and wick materials. The hourly variation of ambient temperature was measured for three configurations of solar still: without wick, with *Strychnos potatorum* wick, and with gooseberry stem wick. The temperature ranged from 28°C to 37°C throughout the day, with the highest temperature being observed in the afternoon. Comparing the configurations, we observe that solar stills with wick materials generally exhibit higher glass, water, and absorber temperatures than the still without wick material. The peak temperatures of the solar still without wick material reached 48°C (glass), 65°C (water), and 66°C (basin), while the still with *Strychnos potatorum* wick material reached 54°C (glass), 66°C (water), and 68°C (basin), and the still with gooseberry wick material reached 52°C (glass), 64°C (water), and 67°C (basin). This outcome is likely due to the improved heat transfer and evaporation rates facilitated by the presence of wick materials. The wick materials, by spreading the water over a larger surface area, enhance the overall heat transfer from solar radiation to the water, promoting faster evaporation. Furthermore, the wick materials can absorb solar radiation, further contributing to the heating of the water. This result suggests that both wick materials are equally effective at enhancing the heat transfer and evaporation processes within the solar stills.

3.3. Hourly distillate output

In this section, we discuss the variation of hourly distillate output for three solar still configurations—without wick, with *Strychnos potatorum* wick, and with gooseberry stem wick—over the course of a day. Distillate output is a critical measure of the performance of solar stills, as it reflects their efficiency in converting solar energy into freshwater through the process of evaporation and condensation. The distillate output for all configurations exhibits a bell-shaped trend, with the peak outputs occurring around solar noon. This pattern can be attributed to the diurnal variation of solar radiation, which results in the highest evaporation rates around midday. The conventional solar still reached a maximum output of 145 mL at 13:00, while the still with *Strychnos* wick and gooseberry wick configurations exhibited peak outputs of 182 and 172 mL, respectively, at 13:00 as shown in Fig. 6. These higher outputs in the *Strychnos* and gooseberry configurations can be ascribed to the wick materials' ability to promote heat transfer and evaporation, as evidenced by our previous temperature analysis. The former configuration consistently outperformed the latter, albeit with only slight differences in distillate output. This observation suggests that the *Strychnos* plant fibers may have a slight advantage over the gooseberry stem fibers in terms of water production efficiency.

3.4. Daily productivity

The daily distillate output of the solar stills, comparing the performance of the still without wick material to those with *Strychnos potatorum* and gooseberry stem wick materials is presented in this section. It can be observed from Fig. 7 that the still with no wick material produced a daily distillate output of 1,053 mL, while the stills with *Strychnos potatorum* and gooseberry stem wick materials generated outputs of 1,632 and 1,494 mL, respectively. The increased distillate output in the stills with wick materials can be attributed to the enhanced heat transfer and evaporation rates facilitated by the wicks. The variation of cumulative yield of all the wick configurations is also presented in Fig. 8. As discussed earlier, the wick materials spread the water over a larger surface area and absorb solar radiation, promoting faster evaporation and increased water production. These materials act as a thermal barrier, minimizing heat loss from the water surface, and allowing for higher evaporation rates and increased water production. The

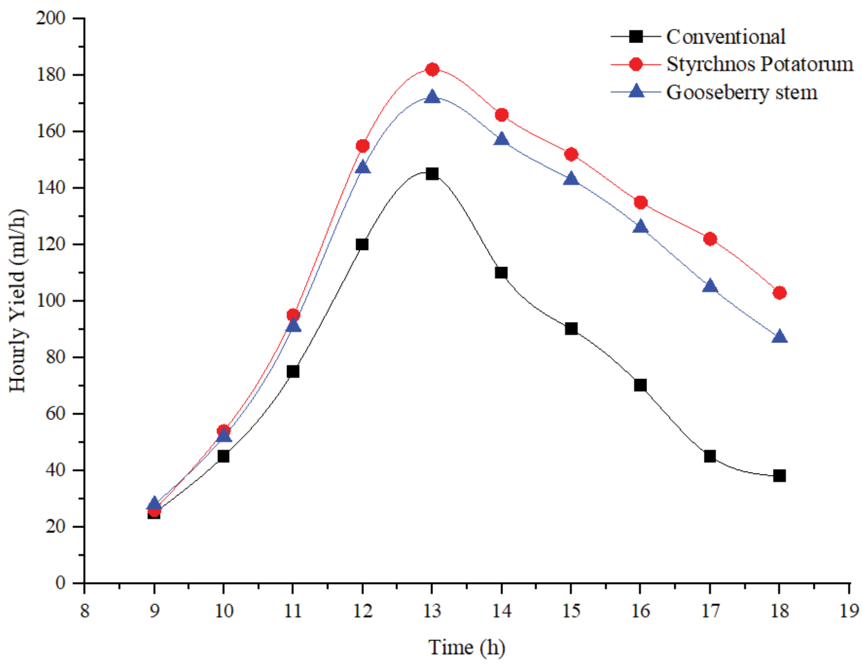

Fig. 6. Variation of hourly yield for various wick configurations.

floating nature of the wick materials also aids in maintaining a thin water layer on the wick surface, which further promotes faster evaporation. Comparing the percentage increase in output, the still with *Strychnos potatorum* wick material displayed a significant improvement of approximately 55%, while the still with gooseberry stem wick material showed a substantial increase of around 42%.

Table 2 depicts the comparison of the present work with recent relevant works based on daily output and cost per litre of freshwater produced.

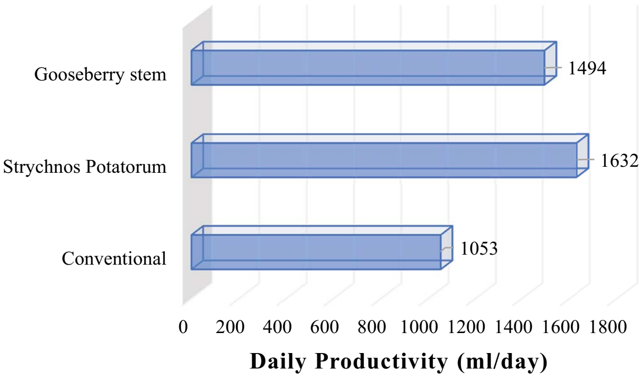

Fig. 7. Daily productivity of solar still with and without wick material.

4. Enviro-economic analysis

In this section, we undertake a multifaceted analysis of the solar still setup featuring natural fiber wick materials, focusing on three key dimensions. First, we conduct an economic analysis to determine the cost per liter of distilled water produced by the system. Next, we examine the exergo-economic factor, evaluating the balance between energy efficiency and economic viability. Lastly, we assess the enviro-economic factor, investigating the environmental impact of the system in conjunction with its financial performance. This comprehensive approach provides a thorough understanding of the system's feasibility, sustainability, and potential contribution to both economic and environmental goals.

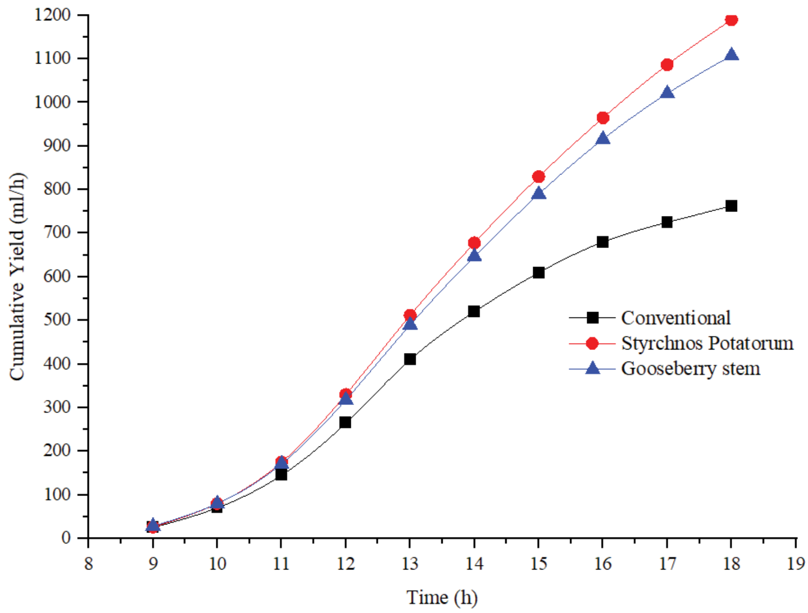

Fig. 8. Cumulative yield of solar still with and without wick materials.

Table 2
Summary of comparison of the present work with other recent works

Type of still	Productivity enhancement (%)	Cost per liter (INR/L)	References
Solar still with gooseberry stem	55	1.44	Present study
Solar still with *Strychnos potatorum*	42	1.30	
Single basin double slope solar still with black cotton wick	75.11	1.95	[35]
Single basin solar still with barrel wick and phase change material with CuO nanoparticles	154	1.78	[36]
Solar still with pond fibers	29.67	1.30	[25]
Convex tubular SS with jute wick over convex absorber	92.5	1.02	[37]

Table 3
Enviro-economic analysis of conventional and modified solar still

Particulars	Conventional solar still	Solar still with gooseberry stem	Solar still with *Strychnos potatorum*
Daily efficiency	31.5%	36.7%	38.4%
Equivalent annual cost (EAC), INR	527.50	644.30	636.48
Yearly yield (L/y)	315.90	448.20	489.60
Cost per liter (CPL), INR	1.67	1.44	1.30
Exergo-economic factor, W/INR	1.16	1.39	1.48
Enviro-economic factor, ton-CO_2/y	0.46	0.64	0.69

4.1. Economic analysis

A key economic parameter for this study is the unit cost of distilled water produced, which accounts for various factors such as the compound interest rate, fixed costs, as well as operation and maintenance expenses throughout the system's anticipated operational period. To conduct a comprehensive cost assessment, we assume 300 working d/y, accommodating potential fluctuations due to climatic variations or unforeseen circumstances during the system's active years.

Cost per litre of the distilled water produced is given by Eq. (6):

$$\text{CPL} = \frac{\text{EAC}}{m_y} \tag{6}$$

where EAC is the equivalent annual cost and is estimated using Eqs. (7)–(10):

$$\begin{aligned}\text{EAC} = &\ \text{Fixed Annual Cost}(\text{FAC}) \\ &+ \text{Annual Maintenance Cost}(\text{AMC}) \\ &- \text{Annual Salvage Value}(\text{ASV})\end{aligned} \tag{7}$$

where

$$\text{FAC} = \text{Capital Cost}(\text{CC}) \times \text{Capital Recovery Factor}(\text{CRF}) \tag{8}$$

$$\text{AMC} = 0.15 \times \text{FAC} \tag{9}$$

$$\text{ASV} = \text{Salvage Value}(\text{SV}) \times \text{Sinking Fund Factor}(\text{SFF}) \tag{10}$$

$$\text{CRF} = \frac{i(1+i)^n}{(1+i)^n - 1} \tag{11}$$

$$\text{SV} = 0.20 \times \text{CC} \tag{12}$$

$$\text{SFF} = \frac{i}{(1+i)^n - 1} \tag{13}$$

The annual rate of interest in India varies from 5% to 8% and the life expectancy of the solar still made of galvanized iron is considered in the range of 10–30 y [31]. The cost comparison of the present study with other related works is presented in Table 3.

4.2. Exergo-economic factor

The exergo-economic factor is a vital metric for researchers, as it enables the optimization of system performance while balancing cost considerations. This factor is calculated by examining the relationship between exergy output and annual payment [32]. Exergy output is preferred over energy in this context, as the solar radiation, a freely available resource with varying availability throughout the year is the primary source of energy input for a solar still. The exergo-economic factor (EXE) is given by Eq. (14):

$$\text{EXE} = \frac{\text{EX}_{\text{out}}}{\text{EAC}} \tag{14}$$

4.3. Enviro-economic factor

The enviro-economic analysis section focuses on quantifying the cost savings achieved through the reduction of CO_2 emissions in the solar still setup with natural fiber wick materials. This factor, known as the enviro-economic factor (ΦEX_{out}, CO_2), is calculated based on the international price of CO_2, currently estimated at $14.5/ton [33].

The enviro-economic factor is given by Eq. (15):

$$\Phi \text{EX}_{\text{out,}}\text{CO}_2 = \Phi \text{CO}_2 \times \varphi \text{EX}_{\text{out,}}\text{CO}_2 \tag{15}$$

where, ΦCO_2 denotes the international price of CO_2, while ΦEX_{out}, CO_2 represents the enviro-economic factor. For ideal plants, CO_2 emissions amount to 0.98 kg/kWh; however, considering system losses, this value increases to 2 kg/kWh.

The environmental factor (φEX_{out}, CO_2) is computed using the Eq. (15):

$$\varphi \text{EX}_{\text{out,}}\text{CO}_2 = \frac{(\text{EX}_{\text{out}} \times N) \times 2}{1000} \tag{15}$$

where φEX_{out}, CO_2 refers to the environmental factor, and N represents the working period expressed in years. By incorporating the enviro-economic analysis into our study, we can comprehensively assess the solar still set-up's environmental and financial benefits, highlighting its potential for sustainable water purification and cost-effective CO_2 emission reduction.

5. Conclusions

In conclusion, this study highlights the significance of incorporating wick materials, namely *Strychnos potatorum* and gooseberry stem, in solar still designs to enhance their performance in freshwater production. The findings indicate that the presence of wick materials improves heat transfer and evaporation rates, resulting in higher temperatures and increased distillate output. Both wick configurations exhibit promising results, with *Strychnos potatorum* showing a slight advantage in water production efficiency. The salient results of the present study are presented below.

- The presence of wick materials facilitated improved heat transfer and evaporation rates. The wicks spread the water over a larger surface area, enhancing overall heat transfer from solar radiation to the water. This, in turn, led to higher temperatures of the basin water in the solar stills.
- The wick materials' ability to promote heat transfer and evaporation processes combined with the thermal barrier effect of the wicks, minimized heat loss from the water surface, resulted in higher evaporation rates and improved water production efficiency. The maximum hourly distillate of 145 mL was observed for the conventional solar while the still with *Strychnos* wick and gooseberry wick configurations exhibited peak outputs of 182 and 172 mL, respectively.
- The still with *Strychnos potatorum* wick material demonstrated a significant increase in the daily productivity of approximately 55%, while the still with gooseberry stem wick material showed a substantial improvement of around 42%. This enhancement can be attributed to the floating nature of the wick materials, which aided in maintaining a thin water layer on the wick surface and promoting faster evaporation.
- Among the three solar still configurations studied, the setup with *Strychnos potatorum* emerged as the most efficient at 38.4%, outperforming the gooseberry stem variant (36.7%) and the conventional setup (31.5%). This heightened efficiency is attributed to its superior yield. Over the day, efficiencies progressively increased, culminating in these values by sunset.
- The cost per liter of freshwater produced with gooseberry stem wick material was 1.39 rupees, while with *Strychnos potatorum* wick material it was 1.48 rupees. This cost reduction can be attributed to the higher distillate outputs achieved with wick materials, indicating a more efficient utilization of resources and supporting the economic viability of incorporating wick materials in solar stills.

Symbols

ε	—	Porosity, %
V_b	—	Bulk volume, m^3
V_s	—	Solid volume, m^3
h	—	Capillary rise, m/h
σ	—	Surface tension of the liquid, N/m
η_d	—	Daily efficiency of solar still, %
θ	—	Contact angle between the liquid and the fibre surface, °
ρ	—	Density of the liquid, kg/m^3
g	—	Gravitational acceleration, m/s^2
r	—	Radius of the capillary, m
W_{rate}	—	Water absorbency rate, s
W_w	—	Final weight of the material after absorbing water, kg
W_d	—	Initial weight of the material before absorbing water, kg
U_x	—	Uncertainty, %
U_n	—	Uncertainty pertaining to the measuring instruments, %
A	—	Base area of the solar still, m^2
h_{fg}	—	Latent heat of vaporization, J/kg
m_w	—	Distillate yield, kg/m^2
I	—	Solar radiation intensity, W/m^2
CPL	—	Cost per litre, INR
EAC	—	Equivalent annual cost, INR
m_w	—	Daily distillate yield, L
η_d	—	Efficiency of solar still, %
h_{fg}	—	Latent heat of vaporization, J/kg
PCM	—	Phase change material
A	—	Base area of the still, m^2
$I(t)$	—	Mean incident solar radiation over the specified duration, W/m^2
FAC	—	Fixed annual cost, INR
AMC	—	Annual maintenance cost, INR
ASV	—	Annual salvage value, INR
CC	—	Capital cost, INR
CRF	—	Capital recovery factor
SV	—	Salvage value
SFF	—	Sinking fund factor
i	—	Interest rate, %
n	—	Number of years
EXE	—	Exergo-economic factor, W/INR
EX_{out}	—	Exergy output
ΦEX_{out}	—	CO_2 enviro-economic factor
ΦCO_2	—	International price of CO_2
φEX_{out}	—	CO_2 environmental factor
N	—	Working period years

References

[1] S.K. Singh, S.C. Kaushik, V.V. Tyagi, S.K. Tyagi, Comparative performance and parametric study of solar still: a review, Sustainable Energy Technol. Assess., 47 (2021) 101541, doi: 10.1016/j.seta.2021.101541.

[2] G. Angappan, S. Pandiaraj, A.J. Alrubaie, S. Muthusamy, Z. Said, H. Panchal, V.P. Katekar, S. Shoeibi, A.E. Kabeel, Investigation on solar still with integration of solar cooker to enhance productivity: experimental, exergy, and economic analysis, J. Water Process Eng., 51 (2023) 103470, doi: 10.1016/j.jwpe.2022.103470.

[3] A. Kulkarni, K. Manohar, G. Hippargi, P.R. Maddigapu, R. Dhodapkar, S.S. Rayalu, Nanophotonics triggered thermally enhanced solar water disinfection bottles for slum dwellers, Environ. Sci. Pollut. Res., 30 (2023) 35269–35280.

[4] D. Sivasankar, S. Subramani, D.K. Murugan, Performance enhancement of single basin solar still using a composite vertical wick configuration, Desal. Water Treat., 282 (2023) 80–85.

[5] M. Elgendi, M. Atef, Calculating the impact of meteorological parameters on pyramid solar still yield using machine learning algorithms, Int. J. Thermofluids, 18 (2023) 100341, doi: 10.1016/j.ijft.2023.100341.

[6] L. Hadj-Taieb, A.S. Abdullah, M. Aljaghtham, A. Alkhudhiri, Z.M. Omara, F.A. Essa, Improving the performance of trays solar still by using sand beds and reflectors, Alexandria Eng. J., 71 (2023) 659–668.

[7] A. Alshqirate, A.S. Awad, A. Al-Alawin, M.A. Essa, Experimental investigation of solar still productivity enhancement of distilled water by using natural fibers, Desalination, 553 (2023) 116487, doi: 10.1016/j.desal.2023.116487.

[8] T.E.M. Atteya, F. Abbas, Testing a stepped solar still with different sand beds and reflectors, Case Stud. Therm. Eng., 43 (2023) 102782, doi: 10.1016/j.csite.2023.102782.

[9] S. Hota, S.S. Hada, C. Keske, G. Diaz, Feasibility of desalination by solar stills for small community scale freshwater demand, J. Cleaner Prod., 379 (2022) 134595, doi: 10.1016/j.jclepro.2022.134595.

[10] G. Lee, C. Park, H. Lim, S. Cho, S. Choi, B. Lim, Performance enhancement of a diffusion-type solar still: wettability and flowability of condensation surface, Renewable Energy, 209 (2023) 277–285.

[11] D.L. Shukla, K.V. Modi, Performance assessment of novel solar still regenerated liquid desiccant-based evaporative air-conditioning system for an office in India, Energy Convers. Manage., 280 (2023) 116813, doi: 10.1016/j.enconman.2023.116813.

[12] N.M. Shatar, M.F.M. Sabri, M.F.M. Salleh, M.H. Ani, Investigation on the performance of solar still with thermoelectric cooling system for various cover material, Renewable Energy, 202 (2023) 844–854.

[13] R. Dhivagar, S. Shoeibi, S.M. Parsa, S. Hoseinzadeh, H. Kargarsharifabad, M. Khiadani, Performance evaluation of solar still using energy storage biomaterial with porous surface: an experimental study and environmental analysis, Renewable Energy, 206 (2023) 879–889.

[14] L.O. Afolabi, C.C. Enweremadu, M.W. Kareem, A.I. Arogundade, K. Irshad, S. Islam, K.O. Oladosu, A.M. Elfaghi, D.H. Didane, Experimental investigation of double slope solar still integrated with PCM nanoadditives microencapsulated thermal energy storage, Desalination, 553 (2023) 116477, doi: 10.1016/j.desal.2023.116477.

[15] S. Senthil Kumar, S.D Uma Mageswari, M. Meena, V. Nagaraju, D.B Yakkala, D.V. Mageshbabu, B. Madhu, R. Sathyamurthy, Effect of energy storage material on a triangular pyramid solar still operating with constant water depth, Energy Rep., 8 (2022) 652–658.

[16] K.V. Modi, A.R. Gamit, Investigation on performance of square pyramid solar still using nanofluid and thermal energy storage material: an experimental and theoretical study, J. Cleaner Prod., 381 (2022) 135115, doi: 10.1016/j.jclepro.2022.135115.

[17] M.Z. Khan, Diffusion of single-effect vertical solar still fixed with inclined wick still: an experimental study, Fuel, 329 (2022) 125502, doi: 10.1016/j.fuel.2022.125502.

[18] M.Z.M. Ahmed, F. Alshammari, A.S. Abdullah, M. Elashmawy, Experimental investigation of a low-cost inclined wick solar still with forced continuous flow, Renewable Energy, 179 (2021) 319–326.

[19] A.S. Abdullah, U. Alqsair, M.S. Aljaghtham, A.E. Kabeel, Z.M. Omara, F.A. Essa, Productivity augmentation of rotating wick solar still using different designs of porous breathable belt and quantum dots nanofluid, Ain Shams Eng. J., (2023) 102248, doi: 10.1016/j.asej.2023.102248.

[20] A.S. Abdullah, L. Hadj-Taieb, Z.M. Omara, M.M. Younes, Evaluating a corrugated wick solar still with phase change material, and external spiral copper heating coil, J. Energy Storage, 65 (2023) 107377, doi: 10.1016/j.est.2023.107377.

[21] M.M.Z. Ahmed, F. Alshammari, U.F. Alqsair, M. Alhadri, A.S. Abdullah, M. Elashmawy, Experimental study on the effect of the black wick on tubular solar still performance, Case Stud. Therm. Eng., 38 (2022) 102333, doi: 10.1016/j.csite.2022.102333.

[22] S.W. Sharshir, M.A. Eltawil, A.M. Algazzar, R. Sathyamurthy, A.W. Kandeal, Performance enhancement of stepped double slope solar still by using nanoparticles and linen wicks: energy, exergy and economic analysis, Appl. Therm. Eng., 174 (2020) 115278, doi: 10.1016/j.applthermaleng.2020.115278.

[23] S.K. Suraparaju, S.K. Natarajan, Performance analysis of single slope solar desalination setup with natural fiber, Desal. Water Treat., 193 (2020) 64–71.

[24] M. Murugan, A. Saravanan, G. Murali, P. Kumar, V.S.N. Reddy, Enhancing productivity of V-trough solar water heater incorporated flat plate wick-type solar water distillation system, J. Heat Transfer, 143 (2020) 032001, doi: 10.1115/1.4048947.

[25] S.K. Suraparaju, R. Dhanusuraman, S.K. Natarajan, Performance evaluation of single slope solar still with novel pond fibres, Process Saf. Environ. Prot., 154 (2021) 142–154.

[26] R.S. Hansen, C.S. Narayanan, K.K. Murugavel, Performance analysis on inclined solar still with different new wick materials and wire mesh, Desalination, 358 (2015) 1–8.

[27] D.K. Murugan, N. Elumalai, Experimental investigation on the time dependant behaviour of productivity of a stacked solar still, Desal. Water Treat., 125 (2018) 1–7.

[28] D.K. Murugan, N. Elumalai, S. Subramani, Experimental investigation on the effect of basin pressure in a single basin solar still, Desal. Water Treat., 229 (2021) 10–16.

[29] A. Rahmani, F. Khemmar, Z. Saadi, Experimental investigation on the negative effect of the external condenser on the conventional solar still performance, Desalination, (2021) 114914, doi: 10.1016/j.desal.2020.114914.

[30] S.W. Sharshir, M.A. Farahat, A. Joseph, A.W. Kandeal, M.A. Rozza, F. Abou-Taleb, A.E. Kabeel, Z. Yuan, Comprehensive thermo-enviroeconomic performance analysis of a preheating assisted trapezoidal solar still provided with various additives, Desalination, 548 (2023) 116280, doi: 10.1016/j.desal.2022.116280.

[31] A.W. Jeevadason, S. Padmini, C. Bharatiraja, A. Elnaby Kabeel, A review on diverse combinations and energy-exergy-economics (3E) of hybrid solar still desalination, Desalination, 527 (2022) 115587, doi: 10.1016/j.desal.2022.115587.

[32] P. Pal, R. Dev, D. Singh, A. Ahsan, Energy matrices, exergo-economic and enviroeconomic analysis of modified multi–wick basin type double slope solar still, Desalination, 447 (2018) 55–73.

[33] A.R. Abd Elbar, M.S. Yousef, H. Hassan, Energy, exergy, exergo-economic and enviroeconomic (4E) evaluation of a new integration of solar still with photovoltaic panel, J. Cleaner Prod., 233 (2019) 665–680.

[34] M.S. El-Sebaey, A. Ellman, A. Hegazy, F.A. Essa, Experimental study with thermal and economic analysis for some modifications on cylindrical sector and double slope, single basin solar still, Case Stud. Therm. Eng., 49 (2023) 103310, doi: 10.1016/j.csite.2023.103310.

[35] P. Pal, P. Yadav, R. Dev, D. Singh, Performance analysis of modified basin type double slope multi–wick solar still, Desalination, 422 (2017) 68–82.

[36] M.M. Younes, A.S. Abdullah, F.A. Essa, Z.M. Omara, Half barrel and corrugated wick solar stills – comprehensive study, J. Energy Storage, 42 (2021) 103117, doi: 10.1016/j.est.2021.103117.

[37] F.A. Essa, W.H. Alawee, S.A. Mohammed, H.A. Dhahad, A.S. Abdullah, Z.M. Omara, Experimental investigation of convex tubular solar still performance using wick and nanocomposites, Case Stud. Therm. Eng., 27 (2021) 101368, doi: 10.1016/j.csite.2021.101368.

[38] S. Rashidi, N. Rahbar, M.S. Valipour, J.A. Esfahani, Enhancement of solar still by reticular porous media: experimental investigation with exergy and economic analysis, Appl. Therm. Eng., 130 (2018) 1341–1348.

[39] M.H. Sharbatiyan, S. Rashidi, M. Mirhosseini, Experimental study on the performance of floating solar desalination system with porous absorber plate, J. Taiwan Inst. Chem. Eng., 148 (2023) 104667, doi: 10.1016/j.jtice.2023.104677.

[40] B. Darbari, S. Rashidi, Performance analysis for single slope solar still enhanced with multi-shaped floating porous absorber, Sustainable Energy Technol. Assess., 50 (2022) 101854, doi: 10.1016/j.seta.2021.101854.